Chromatin-modifying enzymes as modulators of nuclear size during lineage differentiation

Lingjun Meng[1, 2, *]

[1]Department of Pathology,

[2]Institute for Stem Cell Biology and Regenerative Medicine,

Stanford University School of Medicine, Stanford, CA 94305, USA

*Correspondence: lingjun@stanford.edu, menglingjundl@gmail.com.

Key word: histone demethylases, nuclear size, differentiation, cancer.

Abstract

The mechanism of nuclear size determination and alteration during normal lineage development and cancer pathologies which is not fully understood. As recently reported, chromatin modification can change nuclear morphology. Therefore, we screened a range of pharmacological chemical compounds that impact the activity of chromatin-modifying enzymes, in order to get a clue of the specific types of chromatin-modifying enzymes that remarkably effect nuclear size and shape. We found that interrupted activity of chromatin-modifying enzymes is associated with nuclear shape abnormalities. Furthermore, the activity of chromatin-modifying enzymes perturbs cell fate determination in cellular maintenance and lineage commitment. Our results indicated that chromatin-modifying enzyme regulates cell fate decision during lineage differentiation and is

21 associate with nuclear size alteration.

22

23 **Significance**

24 Here we described for the first time the modulation of chromatin-modifying enzymes
25 remarkably effects nuclear shape, and perturbs cell fate determination in cellular maintenance and
26 lineage fate commitment in normal stem cells and leukemia cancer cells. We found that the
27 irregularities of nuclear contour were highly related to pharmacological inhibition of chromatin-
28 modifying enzyme activity. After manipulating a histone demethylase named GASC1, we found
29 that upregulation of GASC1 impairs the differentiation of hESCs to terminally differentiated
30 neural cells. Moreover, upregulation of GASC1 impairs the proliferation of leukemia cells due to
31 cell cycle arrest in the G0/G1 phase and indicates misshapen nuclei. This study suggested that
32 chromatin-modifying enzyme regulates the nuclear contour related cell fate decision also including
33 cancer cell fate determination.

34

35 **Introduction**

36 As reported, nuclear volume is an important morphological parameter that can change during
37 cancer progression (1). After confocal microscopy was discovered and broadly used to observe the
38 detailed structure of specific objects within the cell, the most fascinated cellular organelle - nucleus
39 was researched more carefully. Recent studies have also highlighted that nuclear shape can
40 influence fate decisions (2). Embryonic stem cells (ESCs) differentiation is accompanied by an

41 increase in chromatin condensation (3) leading to an increase in nuclear stiffness (4) and a decrease
42 in nuclear size. As known, the nuclear size of stem cells is extremely bigger than terminal
43 differentiated cells. Cell differentiation is corresponding with chromatin marks reset, which raises
44 the question of whether chromatin's contribution to nuclear mechanics affects nuclear morphology
45 as well as cell fate. It is therefore critical to identify the contributions of various chromatin-
46 modifying enzymes that are relevant to cell fate decisions, and consequently display nuclear size
47 alteration.

48 Nuclear architecture is impacted via chromosome structure which is determined by histone
49 modifications. The cellular differentiation from stem cells to differentiated cells which is
50 corresponding with nuclear size reduction as well as chromosome condense. Histone demethylases
51 have also been reported to be critical enzymes that regulate the balance between self-renewal and
52 differentiation in hESCs (human embryonic stem cells) (5-8). Accordingly, we broadly utilized
53 chromatin-modifying enzymes inhibitors to treat stem cells such as hESCs, NPCs (neural
54 progenitor cells), and later cancer cells such as leukemia cells. We demonstrated that the
55 irregularities of nuclear contour were highly related to pharmacological inhibition of chromatin-
56 modifying enzyme activity. As known, upregulation or downregulation of histone demethylases is
57 observed in various types of cancer and is associated with higher rates of malignancy and relapse
58 after treatment (9). In particular, GASC1 (gene amplified in squamous cell carcinoma, also known
59 as KDM4C, a histone demethylase) promotes chromosomal instability and transcription initiation,
60 therefore, plays a causative role in cancer cells driven by its dysregulation (10). GASC1 was found

61 aberrant expression in esophageal squamous carcinomas (11), medulloblastomas (12), glioma (13),
62 breast cancer (14), and prostate cancer (15). In addition, GASC1 plays an essential role in the
63 transition of mouse ESCs (mESCs) to endothelial cells (16). Consistently, we demonstrated that
64 upregulation of GASC1 impairs the differentiation of undifferentiated hESCs to terminally
65 differentiated neural cells. Moreover, leukemia cells with upregulated GASC1 expression lost their
66 proliferation ability, show cell cycle arrest in the G0/G1 phase, and appear misshapen nucleus.
67 Taken together, epigenetic perturbations are likely to be the cause for misregulation of nuclear size
68 and of certain cancer cell fates (17).
69

70 **Result**

71 **The nuclear size is associated with cell fate decision and chromatin-modifying enzyme**
72 **activity**

73 Size and shape are distinctive aspects of nuclear structure. Nuclear size impacts cell function,
74 and is altered according to the specific status of cell types during cell development (18). It is
75 unclear which modulators effect the altered nuclear size during cell fate transformation. To
76 investigate the distinct nuclear size of various cell types, we employed highly efficient
77 differentiation methods to interrogate the size change of nucleus during lineage differentiation. To
78 differentiate NPCs from hESCs, we used two molecular compounds, SB431542 and LDN193189,
79 to inhibit the TGF-β (transforming growth factor beta) and BMP (bone morphogenetic protein)
80 pathways, which are also called Dual SMAD inhibitors (19). In addition, as we previously used,

81 overexpression of Ngn2 (neural gene neurogenin-2) could converts hESCs into iN cells (induced
82 neuronal cells) with nearly 100% yield in less than two weeks. The hESCs-derived iN cells grow
83 long axons that conduct electrical impulses away from the neuron's cell body (20). We utilized
84 DAPI to stain hESCs for 5 min, then examined the dynamic change of the nuclear size via
85 measuring the area of nucleus under a fluorescence microscope (Fig. 1*A*). Notably, it was shown
86 that there is a reduced size of approximately 40% from hESCs to NPCs, and 24% decrease from
87 NPCs to iN cells (Fig. 1*B*). Consistently as reported, the nuclear size of hESCs is bigger than NPCs,
88 and the nuclear size of NPCs is bigger than iN cells. In addition, it was shown that the nuclear size
89 of hESCs and NPCs are in a wider range than iN cells, which indicates that there is a potential of
90 stem cells in nuclear dynamics. The different sizes of nuclei may correspond with hESCs, NPCs,
91 and neural cells characterized with distinct unique chromatin architecture. During the
92 reprogramming of cell identity and cell fate determination, heterochromatin plays a critical role.
93 H3K9me3 (Tri-methylation of histone H3 lysine 9) is a histone mark associated with
94 heterochromatin, and has emerged as a key player in repressing lineage-inappropriate genes, and
95 shielding them from activation by transcription factors. We investigated the H3K9me3 expression
96 in hESCs and hESC-derived NPCs by immunofluorescence staining. It was shown that there are
97 high levels of expression of H3K9me3 in the nucleus (Fig. 1*C*). To directly address the role of
98 chromatin in nuclear morphology, we employed a range of commercially available chemical
99 compound inhibitors of the enzymes that modulate histone modification state to manipulate
100 chromatin alterations to treat hESCs (Fig. 1*D* and *E*). These available inhibitors of chromatin-

101 modifying enzymes that were represented the various functions of chromatin regulation, which
102 helped us to investigate broadly chromatin-modifying enzymes associated with nuclear alteration.
103 We purchased these inhibitors from tocris as the method shown. As reported, GSK-J1 is a highly
104 potent inhibitor of the H3K27 histone demethylases JMJD3 (KDM6B) and UTX (KDM6A),
105 likewise inhibits KDM5B, KDM5C, and KDM5A to increase H3K27me3. Histone demethylases
106 inhibitor increased heterochromatin levels and chromatin-based nuclear stiffness. Heterochromatin
107 is highly condensed DNA that leads to gene silencing (21). R2HG is oncometabolite produced by
108 mutant isocitrate dehydrogenase 1 (IDH1) and IDH2, inhibits KDM4A in murine embryonic
109 fibroblasts as well as increases H3K9me3, H3K36me3. 5-Aza is a DNA methyltransferase
110 inhibitor that induces demethylation. GSK-LSD1 is a potent and selective lysine specific
111 demethylase 1 (LSD1) inhibitor, increasing H3K4me3, H3K9me3, and H3K27me3. IOX1 is a
112 histone demethylase JMJD inhibitor, increasing H3K36me3, H3K9me3, and H3K27me3. JIB04
113 is a pan Jumonji histone demethylase inhibitor that inhibits H3K4 demethylases, decreases
114 H3K36me3, H3K9me3. NSC636819 is a KDM4A/KDM4B inhibitor, increasing H3K9me3. PBIT
115 is a JARID1 (Jumonji AT-Rich Interactive Domain 1) inhibitor that increases H3K4me3. C646 is
116 a inhibit histone acetyltransferase, which corresponds predominantly to decompacted euchromatin,
117 allowing transcription factors to bind to regulatory sites on DNA, in order to cause transcriptional
118 activation (22). Through the treatment with compounds function as chromatin-modifying enzyme
119 inhibitors, we found that 5-Aza treatment enlarges the nuclear size of hESCs remarkably (Fig. 1*D*),
120 also some other inhibitors. The great increase in nuclear size of hESCs from 5-Aza treatment

121 indicated that modulation of chromatin-modifying enzymes is enabled to change nuclear size (Fig.
122 1*E*). It suggested that perturbation of chromatin-modifying enzyme activity alters nuclear size in
123 normal cells.

124 In addition, we noticed that the treatment of high concentrations of IOX1 revealed the
125 cytotoxic effects on hESCs. Therefore, we tested a series of concentrations of compounds for
126 hESCs treatment. The high concentrations of inhibitors caused cell death of hESCs, such as 100
127 mM GSK-J1, 100 mM IOX1, 1 mM JIB04, 10 mM PBIT, 25 mM C646, especially, 10 μM, 1 mM,
128 10 mM 5-Aza induced numerous of hESCs death. The high concentrations of inhibitors have
129 cytotoxic effects on cells and impact cells alive. However, hESCs grow well in 60 μM, 1 mM, 10
130 mM GSK-J1, 100 mM R2HG, 10 mM and 100 mM GSK-LSD1, 1 mM and 10 mM IOX1, 10 μM
131 and 100 μM JIB04, 10 μM and 10 mM NSC636819, 100 μM and 1 mM PBIT, 250 μM and 2.5
132 mM C646 treatment. It indicated that compounds function as chromatin-modifying enzyme
133 inhibitors which effect nuclear size alteration, possibly through modulating histone dynamics. It
134 had been shown that utilizing histone methyltransferase inhibitors to decrease heterochromatin
135 results in a softer nucleus and nuclear blebbing, without perturbing lamins. Histone demethylase
136 inhibitors increase heterochromatin and chromatin nuclear rigidity (23). Given that measurements
137 in these reports demonstrate that there is evidence that nuclear size abnormalities can be caused
138 by alterations to chromatin regulatory proteins.

139

140 **Inhibition of chromatin-modifying enzyme effects nuclear size and cell identification of NPCs**

141 Not only hESCs, but we also found that the treatment of 5-Aza, C646, and JIB04 enhanced the
142 nuclear size of hESC-derived NPCs. In contrast, the treatment of R2HG, GSK-LSD1, NSC636819,
143 IOX1 reduced the nuclear size of hESC-derived NPCs (Fig. 2*A*). 5-Aza treatment slightly reduced
144 the nuclear size of hESC-derived iN cells (Fig. 2*B*). To gain further insights into whether these
145 inhibitors not only impact nuclear size and cell death but also effect additional features, such as
146 cell fate decisions, we treated the hESC-derived NPCs with DMSO and chromatin-modifying
147 enzyme inhibitors. The concentration we used was tested and the same concentration was used as
148 hESCs treatment, then imaged hESC-derived NPCs after staining for Sox1 (green), PI (red), and
149 DAPI (blue) (Fig. 2*C*). As known, Sox1 is a neural stem cell marker and is highly expressed in
150 NPCs. It was observed that the expression of Sox1 was significantly reduced in a large number of
151 NPCs in 5-Aza, JIB04, PBIT, GSK-J1, GSK-LSD1, c646, and IOX1 treatment (Fig. 2*D*). To
152 eliminate the possibility of Sox1 expression decrease caused by cell death, we performed
153 propidium iodide (PI) staining to NPCs after inhibitors treatment. As known, PI is not permanent
154 to live cells but is used to detect dead cells in a population. It was shown that Sox1 silence was not
155 caused by cell death due to PI staining being negative. Except IOX1, JIB04 and GSK-LSD1
156 increased PI staining in NPCs which suggested that it may induces cytotoxic responses of NPCs
157 occur as a consequence of cell death. Therefore, it suggested that the compound inhibitors of
158 chromatin-modifying enzymes perturb cell identification. Collectively, inhibition of chromatin-
159 modifying enzymes activity enabled to impact nuclear size in both hESCs and NPCs which
160 consequently leads cell fate to aberrant states.

161

162 **Upregulated GASC1 impairs differentiation from hESCs to iN cells**

163 As we previously discussed, the nuclear size dramatically reduced from hESCs to NPCs, and
164 to iN cells during lineage differentiation. Additionally, we want to validate the specificity of the
165 targeted chromatin-modifying enzyme instead of using chemical compounds. So, we selected three
166 represented histone enzymes such as GASC1, DNMT3A, and KDM4A, based on the screening of
167 inhibitors of chromatin-modifying enzyme activity, to investigate the impact of chromatin-
168 modifying enzymes in lineage differentiation. GASC1 (lysine-specific demethylase 4C, KDM4C)
169 is a histone demethylase as well as KDM4A (lysine-specific demethylase 4A), they both belong to
170 the families of lysine demethylases (KDM). DNMT3A (DNA methyltransferase 3A) catalyzes 5-
171 methylcytosine methylation. 5-Aza inhibits DNA methyltransferase (DNMT). We used the
172 doxycycline (dox)-inducible lentiviral vector system to transduce empty vector plasmid as control
173 and GASC1, DNMT3A, KDM4A into the hESCs H1 cell line, separately. As mentioned above,
174 we used the same approach to induce neuronal cells from differentiating hESCs by Ngn2
175 overexpression (20). It was shown that there is a significantly high efficiency of wt hESCs
176 differentiating to iN cells as nearly 100%. The iN cells display a mature neural morphology with
177 axon extension and packaged smaller cell nucleus (Fig. 3*A*). We stained hESC-iN cells with a
178 neuronal marker Tuj1 (tubulin beta-III) and a pluripotent marker Sox2. It demonstrated that iN
179 cells differentiated from wt hESCs showed Tuj1 positive expression and long axon extension, no
180 Sox2 indicated hESCs left, which also occurred in KDM4A overexpressed hESC-iN cells. In

181 contrast, hESC-iN cells with induced overexpression of GASC1 and DNMT3A that grew few
182 extend axons and showed big nuclei. In addition, a large number of cells were Sox2 positive during
183 differentiation (Fig. 3*A*). After measurement analysis of neurite length at 14 days of iN cell
184 differentiation, we found that hESC-iN cells with GASC1 and DNMT3A overexpression grew
185 remarkably shorter neurite compared to wt and KDM4A overexpressed iN cells (Fig. 3*B*).
186 Perturbation of chromatin-modifying enzymes activity alters the molecular and cellular identity of
187 stem cells. Overall, these data suggested that chromatin-modifying enzymes can drive lineage
188 specification as well as assist nuclear reconstruction, in order to facilitate a smoother transition
189 from stem cells to differentiated cells.
190

191 **GASC1 promotes aberrant nuclear structure and cell cycle arrest of leukemia cells**

192 As above discussed, chromatin-modifying enzyme activity is highly associated with nuclear
193 size alteration in normal stem cells during lineage differentiation. As reported, cancer cells are
194 known to develop larger nuclei as they become more malignant and increase the nuclear-to-
195 cytoplasmic ratio (24). The mechanisms that underlie the increase in nuclear size in malignant
196 cells remain largely unknown. Abnormal nuclear morphology has been used for cancer diagnoses
197 for nearly a century in tests such as the Pap smear (25). We measured the nuclear size of K562
198 leukemia cells by DAPI staining, in order to investigate the distinctive features of chromatin-
199 modifying enzyme activity in cancer cells compared to normal stem cells (Fig. 4*A* and *B*). We
200 tested a series of concentrations of compound inhibitors for K562 cells treatment. Consistent with

201 hESCs, high concentrations of inhibitors caused cell death of K562 cells. Especially, high doses
202 and long-time of 5-Aza and PBIT treatment induce cell death. In addition, we photographed the
203 DAPI stained nucleus of K562 cells treated with DMSO as control and 5-Aza, IOX1, GSK-LSD1,
204 and JIB04. It was shown that K562 cells treated with inhibitors have a bigger size of nucleus and
205 twisted shape as clover, especially in 5-Aza, IOX1, GSK-LSD1, and JIB04 treatment (Fig. 4*A*). It
206 demonstrated that the irregularity of nuclear contour occurred in inhibitors treatment from the
207 visible fluorescent images. The most studied types of nuclear morphological abnormalities are
208 protrusions from the normally ellipsoidal nucleus, termed "blebs." K562 cells showed a "blebs"
209 shape and seem to prefer to have a twisted nuclear shape but not die as quickly as hESCs and NPCs
210 did. It all suggested that not only nuclear size change but also nucleus misshapen are indicated the
211 pathological change of K562 leukemia cells induced by inhibition of chromatin-modifying enzyme
212 activity. Furthermore, the size of cancer cells was more similar to hESCs but bigger than NPCs.
213 After inhibitors treatment for 7 days (10 μM GSK-J1, 100 μM R2HG, 1 μM 5-Aza, 10 μM GSK-
214 LSD1, 10 μM IOX1, 100 μM JIB04, 10 μM NSC636819, 1 μM PBIT, 2.5 μM C646), compared
215 to DMSO control, the increased percentage of nuclear size of K562 cells is 5% ~ 44%. The
216 treatment of 5-Aza and IOX1 markedly lead to the enlargement of the nuclear size of K562
217 leukemia cells (Fig. 4*B*). Except for lamina perturbation affecting nuclear abnormalities (26), it
218 also suggested that enlarged and twisted nuclear size effect the survival of K562 cells which is
219 associated with chromatin-modifying enzyme activity.

220 As mentioned above, these chromatin-modifying enzymes effect lineage differentiation of

221 hESCs. These hESC-iN cells with GASC1 and DNMT3A aberrant expression retain their
222 proliferation capability, fail to differentiate, and acquire resistance to cell death (Fig. 3). As
223 previously reported, IDH1 mutated cells generate R(2)-2-hydroxyglutarate (2HG) (27), which
224 causes GASC1 mediated hypermethylation (15, 28). IDH1 gene mutations occur frequently in
225 AML (acute lymphoblastic leukemia). Accordingly, we investigated the role of GASC1 in K562
226 leukemia cells differentiation. Basically, healthy K562 cells are spherical in shape without any
227 structural distortions, and grow in suspension (Fig. 4*C*). After being differentiated by Ngn2
228 overexpression for 14 days, it was shown that a portion of K562 cells grew spike, and Tuj1 was
229 not abundantly expressed (Fig. 4*C*). K562 cells are hard to differentiate. When adding dox in cell
230 culture for inducing GASC1 overexpression, the majority of K562 leukemia cells began to change
231 their morphology from smooth surfaces of spherical shape to twisted cellular shape compared with
232 no dox-induced K562 cells (Fig. 4*D* and *E*). The abnormal nuclear morphology and protrusions
233 termed "blebs" are both associated with chromatin alterations (23). To validate the cell shape
234 change corresponding to nucleus change, we stain K562 cells with DAPI. Under microscope
235 examination of GASC1 overexpressed K562 cells with or without dox, we found that it is
236 consistent with cell shape change in dox-induced overexpressed K562 cells, that showed nucleus
237 enlarges and shapes as clover (Fig. 4*F* and *G*). To investigate whether the twisted shape
238 consequently provides benefits of growth of the K562 cells or not, we employed the BrdU cell
239 proliferation assay to interrogate the cell cycle of K562 cells growth. The dox-induced K562-
240 GASC1 cells significantly proliferate slower than the no dox-induced K562-GASC1 cells (Fig. 4*H*

241 and *I*). Meanwhile, we count the cell number of K562 cells with or without dox-induced GASC1
242 overexpression, it reveals that there is a significant reduction in the growth of K562 cells with
243 GASC1 overexpression (Fig. 4*J*). To explore the mechanism of K562 cells with GASC1
244 expression was able to stop proliferation at the genetic level, we selected a range of key regular
245 genes function as cell cycle effectors, such as Rbl2, PRDM1, p21, p53, E2F4, lin9, and CDK2 (29,
246 30, 31). Based on the qPCR results, we found that there is a remarkably increased transcription
247 level of Rbl2, PRDM1, p21, E2F4, lin9, and CDK2 in the dox-induced GASC1 expression K562
248 cells than in no dox cells (Fig. 4*K*). p53 mRNA level was reduced markedly in the dox-induced
249 GASC1 expression K562 cells. As known, depletion of p53 in cells causes G1 arrest and apoptosis.
250 Taken together, modulation of GASC1 expression in leukemia cells leads to cell cycle arrest in the
251 G0/G1 phase and shows misshapen nuclei. Through regulating the activity of chromatin-
252 modifying enzymes, that lead to nuclear rupture and blebs, we sought to address a novel strategy
253 to regulate cancer cell growth.
254

255 **Discussion**

256 The objective of this study was to investigate the manner in which both cellular and nuclear
257 size change during differentiation and how such changes might relevant to chromatin-modifying
258 enzymes. However, to date, there have not been many investigations of chromatin contribution to
259 nuclear morphology, although altered histone modifications and chromatin decompaction are
260 consistently present in both nuclei with abnormal morphology and nuclear blebs.

261 Lamins are fibrous proteins as well as nuclear structural proteins. Mouse ES cells express high
262 levels of A-type lamin during cell differentiation (32, 33). Forced expression of the progerin mutant
263 isoform of lamin A/C (LMAC) increases osteogenic differentiation and reduces adipogenic
264 differentiation (33). Additionally, deregulation of lamin expression can lead to various cancer and
265 be used as diagnostic biomarkers. Lamin is a genetic reason for nuclear misshapen, however
266 epigenetic mechanism of nuclear shape change in cell fate determination is still obscure. Here, we
267 aim to understand whether activity alterations of chromatin-modifying enzymes affect nuclear
268 contour, and what mechanisms contribute to cellular identification of cell fate. We employed
269 histone-modifying enzyme inhibitors to get some clues of whether certain types of enzymes or all
270 histone-modifying enzymes are able to effect nuclear size alteration. We used stem cells such as
271 hESCs and NPCs to investigate the impact of histone-modifying enzyme inhibitors at the stage of
272 pluripotency and multipotency maintenance, which may have some distinctions. Also, we
273 investigated the impact of histone-modifying enzyme inhibitors on cancer cells such as leukemia
274 cells. We observed that there is enlarged nuclear size and misshapen nucleus via chromatin-
275 modifying enzyme inhibition. As known, heterochromatin appears larger, fewer, and decondensed
276 in ES cells, numerous and condensed in ES cell-derived neuronal progenitor cells, and appear
277 fewer but more compact in terminally differentiated neurons (34, 35). Additionally, cancer cells
278 have global alterations in chromatin organization, mostly a reduction in heterochromatin (36).
279 Therefore, it suggested that the original histone states identify the specific type of cell, and impact
280 the outcome of histone-modifying enzymes inhibitors treatment.

281 In addition, when treated with histone-modifying enzyme inhibitors, the nuclear size was able
282 to alter, and the nuclear shape becomes aberrant. It demonstrated that chromatin state is a major
283 factor determining the morphology of the nucleus. The increase of nuclear blebbing in nucleus
284 which indicated that a consequence of increasing euchromatin or decreasing heterochromatin, and
285 decreasing nuclear rigidity. In addition, during dysregulation of histone by treatment of histone-
286 modifying enzyme inhibitors, some cells were unable to endure the stimulation and die, but some
287 cells with a misshapen nucleus survived. Is that the reconstructive chromatin provides certain
288 benefits for cell survival during chromatin-modifying enzyme dysregulation? After treatment of
289 histone-modifying enzyme inhibitors in NPCs, it was shown that the decreased expression of genes
290 who play a role in stem cell identification. We also observed the nuclear size become smaller and
291 smaller when cells were differentiated from hESCs to NPCs, then to iN cells. Simultaneously,
292 chromatin appears decondensed in ES cells, then appears more compact in differentiated neurons.
293 Collectively, it implies that the major function of chromatin-modifying enzyme is to determine cell
294 fate, nuclear size alteration is a phenomenon accompanied by the occurrence of cell lineage
295 commitment in normal cells.

296 As known, histone modifications correlate with ESC differentiation. Hundreds of promoters
297 of pluripotent genes gain their epigenetic marks, whereas many others lose it, during the transition
298 from ESC to NPCs, and from NPCs to differentiated neurons (37, 38). Through modulating
299 chromatin-modifying enzymes that are able to control a huge number of epigenetic marks on the
300 promoters of stem cell genes. Therefore, we ask for is that possible to modulate chromatin-

301 modifying enzymes to alter cancer cell fate. We selected three representative chromatin-modifying
302 enzymes. Unlike KDM4A-B, KDM4C (GASC1) is associated with chromatin during mitosis, and
303 triggers the demethylation of H3K9me3 mark (10). Ectopic expression of GASC1 or other JMJD2
304 members markedly decreases H3K9me3/me2 levels, increases H3K9me1 levels, delocalizes HP1
305 (heterochromatin protein 1), and reduces heterochromatin in vivo (15). GASC1 is an Oct4 target
306 in mouse ES cells, and acts as a positive regulator of Nanog, also is preferentially expressed in
307 undifferentiated ES cells (8, 39). Depletion of GASC1 in ES cells induced differentiation with a
308 global increase in H3K9me3, confirming that the histone demethylase activity of GASC1 is linked
309 to the maintenance of pluripotency. The expression levels of GASC1 were also significantly related
310 to the grade of basal-like breast cancers which is the most aggressive type (14). It suggested that
311 histone-modifying enzymes impact the cell fate of normal cells as well as cancer cells. To
312 investigate the impact of GASC1 in cancer cells, we manipulated GASC1 expression in a
313 commonly used leukemia cell line K562. We found that overexpression GASC1 impairs the cell
314 cycle process, deprives K562 cells proliferation capacity, and shows nuclear abnormalities. It
315 indicated that chromatin-modifying enzymes are associated with nuclear size determination and
316 cell fate decision of normal cells as well as cancer cells. Through modulating chromatin-modifying
317 enzymes activity which enables to deprive the aggressive proliferation capacity of cancer cells,
318 arrest cells in the cell cycle to die, and as a consequence, show nucleus misshapen.
319
320 **Methods**

321 **Cell culture and media.**

322 All cell types were maintained at 37°C in a humidified 5% (vol/vol) CO2 environment during
323 culture. H1 ES cells were obtained from WiCell Research Resources (WiCell, WI). ES cells were
324 maintained as feeder-free cells in mTeSR™1 medium (Stem Cell Technologies). Cells were
325 allowed to spread overnight prior to transduction. We used a doxycycline (dox)-inducible lentiviral
326 vector system to transduce empty vector plasmid as a control and GASC1, DNMT3A, KDM4A
327 into the H1 ES cells, separately. Selection was carried out for 7 days in mTeSR™1 medium with
328 50 μg/ml hygromycin.

329 **Generation of iN cells from human ES cells**

330 H1 human ESCs were dissociated using accutase and plated as single cells in mTeSR™1 medium
331 supplemented with ROCK inhibitor Y-27632 (10 μM, StemCell Technologies, Inc.) on matrigel to
332 a final density of 20,000-30,000 cells per cm^2. On the second day, attached cells were infected with
333 lentivirus for Ngn2-puro and rtTA expression. After 24 hr (day 0), transgene expression was
334 induced by replacing the medium with N2/B27 medium (DMEM/F12, N2 supplement (Life
335 Technologies), B27 supplement (Life Technologies), 10 μg/ml insulin (Life Technologies)), and
336 2 μg/ml Doxycycline. Selection was carried out for 14 days (day 1 to day 14) in N2/B27 medium
337 with 2 μg/ml puromycin. From day 2, induced neuronal cells were maintained in N2/B27 medium
338 and changed medium every 2 days.

339 **hESCs differentiate to neural progenitor cells**

340 Growing hESCs in mTeSR media on matrigel coated dish until confluent, then enzymatically

341 passage with accutase, resuspend in Neurobasal-A medium, DMEM/F12, 1% N2, 1% B27 and
342 insulin media, with Y-27632, a specific inhibitor of Rho kinase activity, cultured in the same size
343 of the dish without matrigel coated. Overnight, colonies will form floating spherical clusters
344 termed "embryoid bodies" (EBs). Wait until the EB size grows to 200～400 μm, gently move it to
345 matrigel coated dish. The next day, it will attach to the bottom. Changing medium with N2/B27
346 media supplemented with dual SMAD inhibitors (LDN193189 and SB431542). Feed EBs every
347 second day with N2/B27 media supplemented with 0.1 μM LDN193189 and 10 μM SB431542.
348 After several days, the neural rosettes begin to appear, characterized as round clusters of
349 neuroepithelial cells with apicobasal polarity. Staining Sox1 to indicate the neural progenitor cells.

350 **Virus generation**

351 Lentiviruses were produced as described (40) in HEK293T cells (ATCC, VA) by co-transfection
352 with three helper plasmids (pRSV-REV, pMDLg/pRRE and vesicular stomatitis virus G protein
353 expression vector) (12 μg of lentiviral vector DNA and 6 μg of each of the helper plasmid DNA
354 per 75 cm^2 culture area) using calcium phosphate (41). Lentiviruses were harvested with the
355 medium 24 and 46 hr after transfection. Viral supernatant was filtered through a 0.45 μm filter,
356 pelleted by centrifugation (21,000 × g for 2 hours), resuspended in DMEM, aliquoted, and snap-
357 frozen in liquid N_2. Only virus preparations with >90% infection efficiency as assessed by EGFP
358 expression or puromycin resistance were used for experiments.

359 **Lentiviral infections**

360 Complementary DNAs for candidate genes were cloned into doxycycline-inducible lentiviral

361 vectors, as described previously (42). Lentiviral production and cell infection were performed as
362 described previously (43). Cells were infected with concentrated lentivirus and treated with
363 doxycycline (2 mg/ul) 16-24 h later.

364 **Immunofluorescence**

365 Cultured iN cells were fixed in 4% paraformaldehyde in PBS for 15 min at room temperature,
366 washed three times with PBS, and incubated in 0.2% Triton X-100 in PBS for 10 min at room
367 temperature. Cells were blocked in PBS containing 10% BSA for 3 hours at 4℃. Primary
368 antibodies were applied overnight. Cells were washed in PBS three times. Secondary antibodies
369 were applied for 3 hours, washed. 300 nM DAPI staining for indication of nucleus. Mount.

370 **Antibody**

371 The following primary antibodies with indicated dilution in blocking buffer were used: Rabbit
372 anti-Tuj1 (Covance, BioLegend, MRB-435P, 1:1,000), Mouse anti-Tuj1 (Covance, BioLegend,
373 MMS-435P, 1:1,000), Rabbit anti-human Sox1 (Millipore, AB15766, 1:200), Goat anti-Sox2
374 (Santa Cruz, 1:200). After staining with corresponding secondary antibodies in PBS plus 1% BSA,
375 coverslips were washed four times with PBS, each for 10 min, mounted with the mounting medium
376 onto glass slides, and examined under Olympus FluoView FV1000.

377 **Inhibitors of chromatin-modifying enzymes**

378 Purchase from tocris. GSK J1 (Cat. No. 4593), (R)-2-Hydroxyglutaric acid disodium salt (R2HG,
379 Cat. No. 6124), GSK-LSD 1 dihydrochloride (Cat. No. 5361), IOX 1 (Cat. No. 4464/10), JIB04
380 (Cat. No. 4972/10), NSC636819 (Cat. No. 5287/10), PBIT (Cat. No. 5930), C646 (Cat. No.

381 4200/10), 5-azacytidine (5-Aza, Cat. No. 3842).

382 **qRT-PCR**

383 RNA was isolated through standard methods following manufacturer's instructions (QIAGEN),
384 and reverse transcribed with Superscript III (Life Technology). qRT-PCR was performed with Fast
385 Start universal SYBR green master mix (Roche) along with gene specific primers on a 7900HT
386 real-time PCR machine (Applied Biosystems). Statistical significance was determined by Students
387 t test based on triplicated experiments.

388 **Statistical Tests**

389 Microsoft Excel was used for data analysis. Cumulative plots were generated from parameters
390 collected from individual cells under similar experimental conditions. Average data are presented
391 as bar graphs indicating means ± SD. Statistical comparisons between bar graphs were made using
392 the unpaired, two-tail, Student t test (*$P < 0.05$, **$P < 0.01$, and ***$P < 0.001$, all versus control).

Acknowledgements

I would like to thank all our laboratory members and collaborators for their comments and dedicated work that have greatly contributed to the ideas presented here.

Author Contributions

L.M. conceived and designed the study; L.M. planned and performed the experiments; L.M. wrote the manuscript.

Declaration of Interests

The authors declare no conflicts of interest in the presented study.

403 **FIGURE LEGENDS**

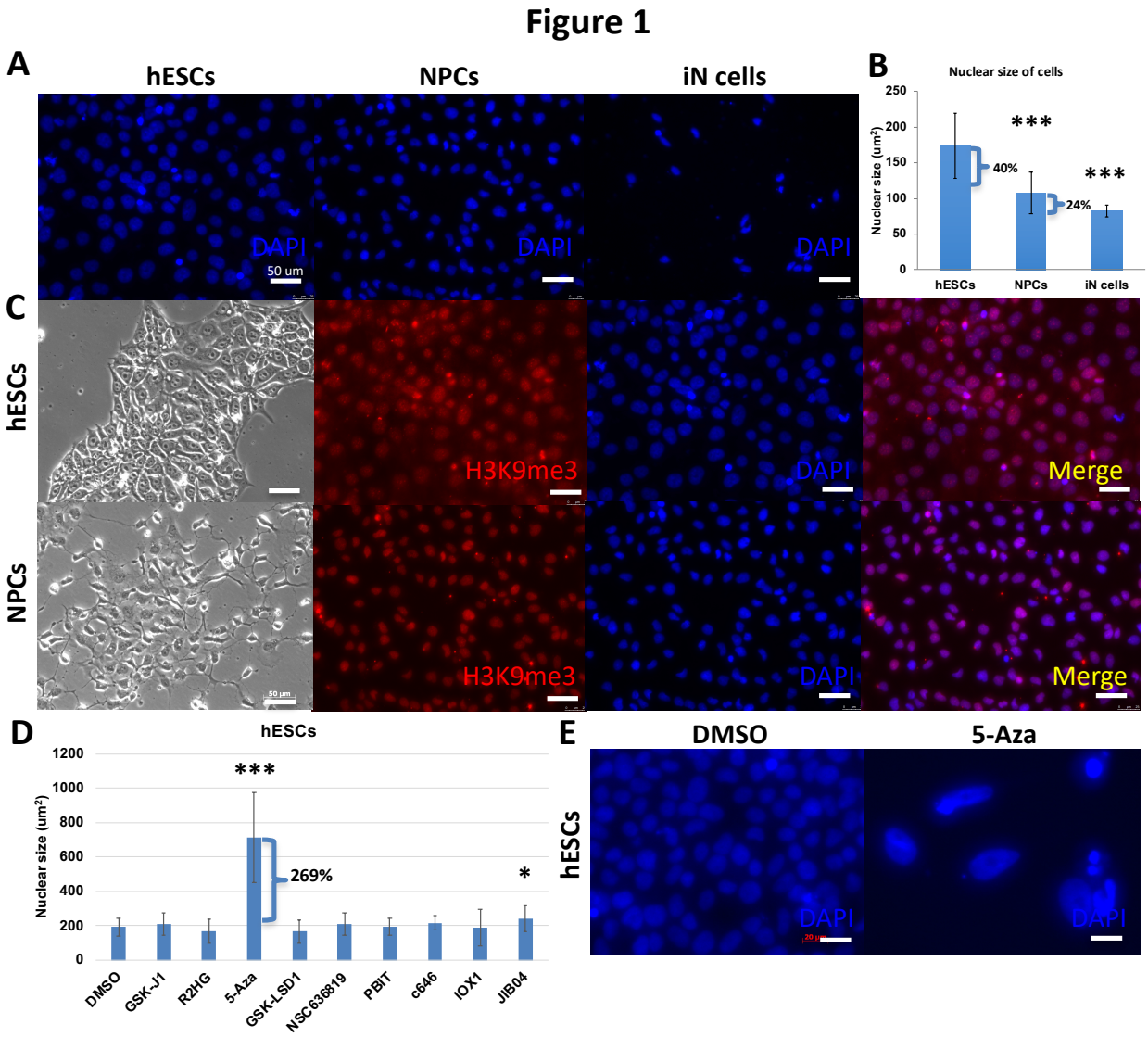

404

405 **Fig. 1. Nuclear size is associated with cell fate decision and chromatin-modifying enzyme**

406 **activity.**

407 **(*A*)** Immunofluorescence staining cell nucleus of hESCs, hESC-derived NPCs, hESC-derived iN

408 cells by DAPI (blue). White scale bars= 50 µm.

409 **(*B*)** Measurements of cell nucleus size of hESCs, hESC-derived NPCs, hESC-derived iN cells by

410 DAPI staining. ***P < 0.001.

411 **(*C*)** Brightfield and fluorescent images of hESCs and hESC-derived NPCs immunofluorescence

412 staining for H3K9me3 (red) and DAPI (blue).

413 **(*D*)** Measurements of nuclear size after hESCs treated with histone demethylase inhibitors (GSK

414 J1, (R)-2-Hydroxyglutaric acid disodium salt, GSK-LSD1, NSC636819, PBIT, IOX1, JIB04),

415 DNA methyltransferase inhibitor (5-Azacytidine), and histone acetyltransferase inhibitor (C646)

416 by DAPI staining. Statistically significant differences are marked with asterisks. *P < 0.05, ***P

417 < 0.001.

418 **(*E*)** Representative immunocytochemistry images of hESCs stained with DAPI. hESCs treated

419 with DMSO as control and 5-Aza. It was shown that the bigger nuclei occurred at 5-Aza treatment.

420 The images were taken at 40× on a confocal microscope. White scale bars= 20 μm.

Figure 2

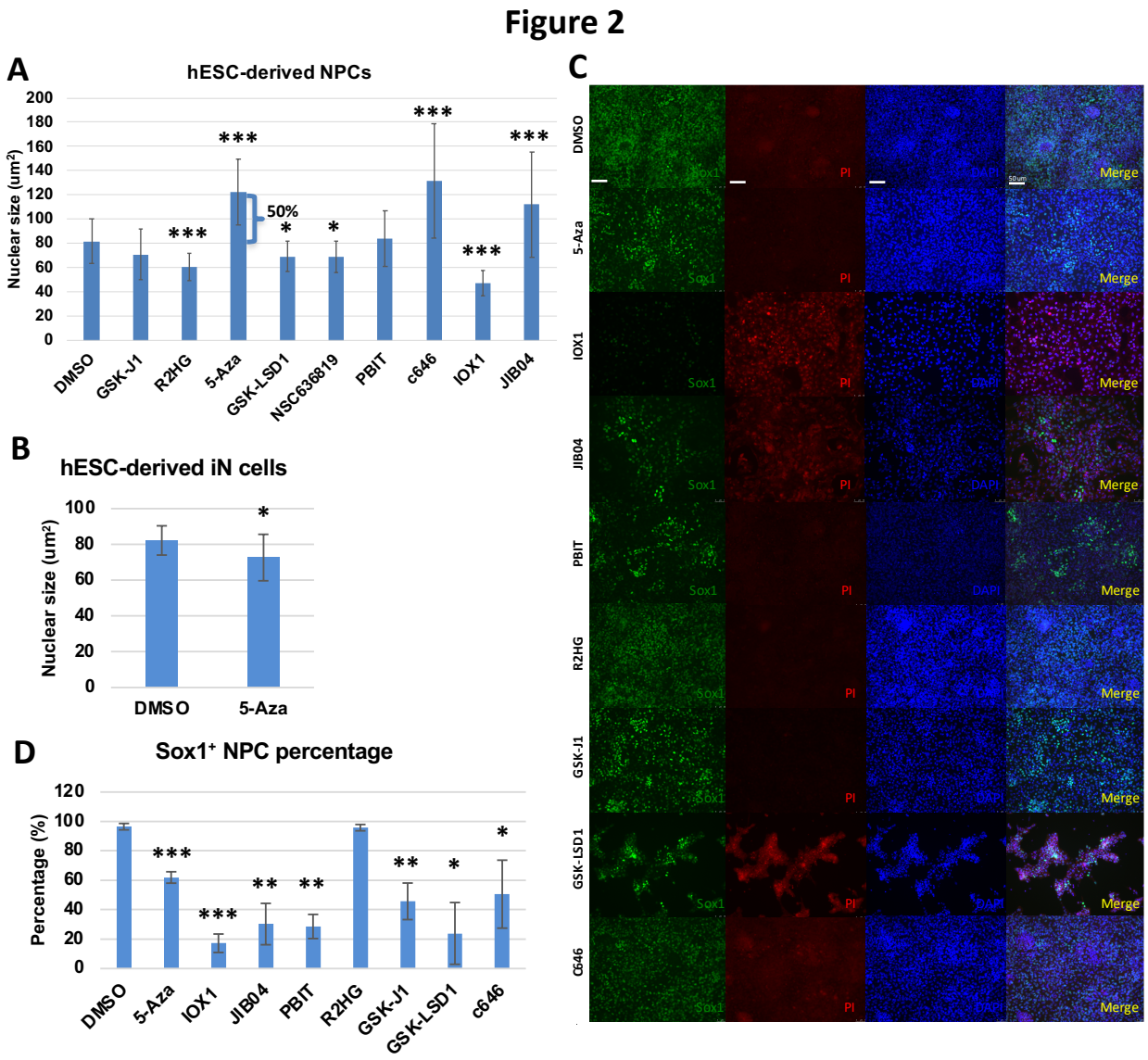

Fig. 2. Inhibition of chromatin-modifying enzyme effects nuclear size and cell identification of NPCs.

(***A***) Measurements of nuclear size by DAPI staining after hESC-derived NPCs treated with DMSO as control and chromatin-modifying enzymes inhibitors.

(***B***) Measurements of nuclear size by DAPI staining after hESC-derived iN cells treated with DMSO as control and 5-Aza.

428 **(*C*)** Fluorescent images of hESC-derived NPCs immunofluorescence staining for Sox1 (green), PI

429 (red), and DAPI (blue) after treatment with DMSO as control and inhibitors of chromatin-

430 modifying enzymes. White scale bars= 50 µm.

431 **(*D*)** Percentage of cells expressing Sox1 (green) over DAPI (blue) total cells. *P < 0.05, **P <

432 0.01, ***P < 0.001.

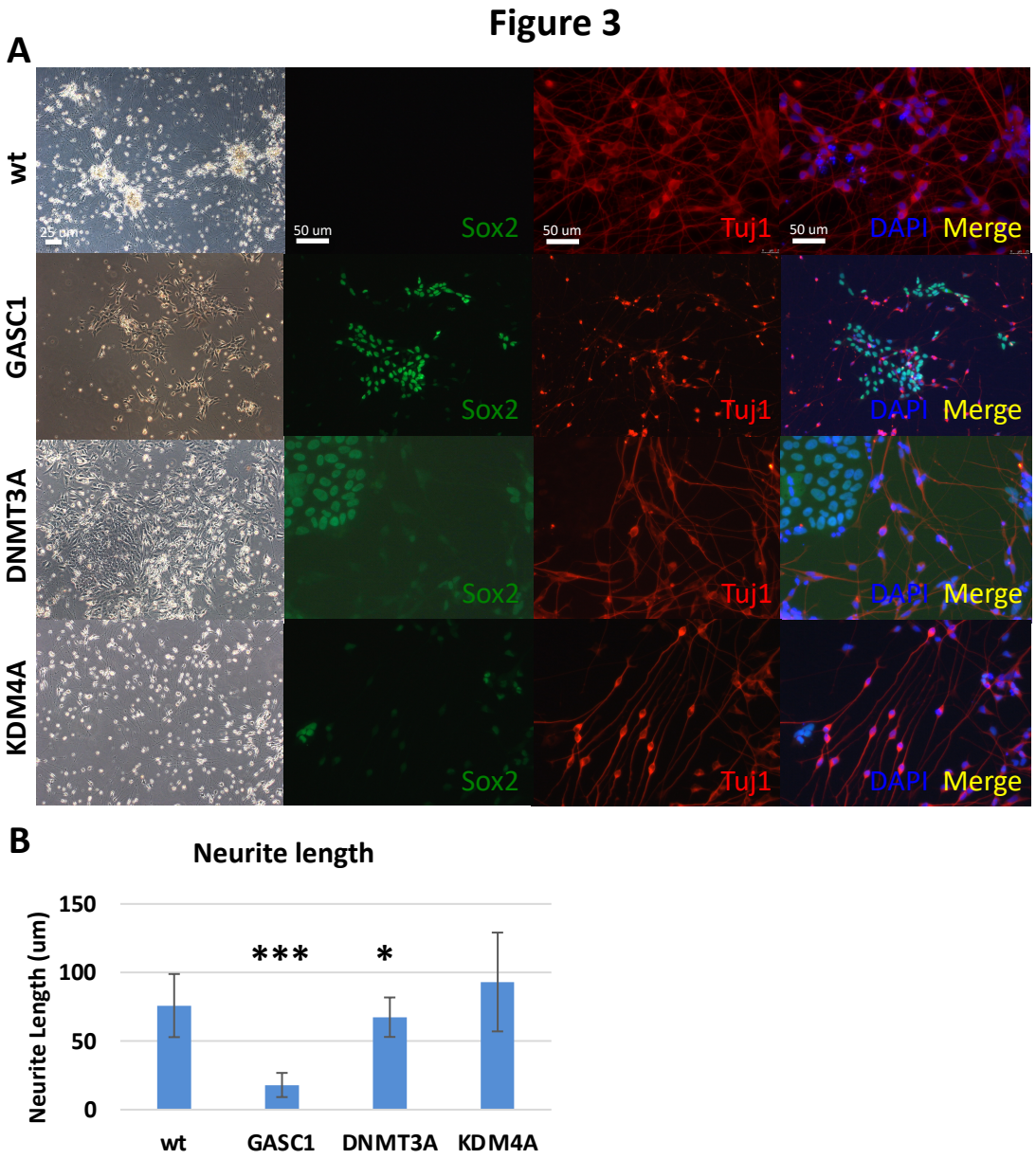

433

434 **Fig. 3. Upregulated GASC1 impairs differentiation from hESCs to iN cells.**

435 **(*A*)** Brightfield and fluorescent images of hESC-derived iN cells with wt, dox-induced

436 overexpression of GASC1, DNMT3A, and KDM4A stained for the pluripotent marker Sox2

437 (green), the neural cells marker Tuj1 (red), and nucleus staining DAPI (blue) after 14 days of iN

438 cells differentiation.

439 **(*B*)** Neurite length of hESC-derived iN cells was measured at 14 days of iN cells differentiation.

440 p-values were calculated by unpaired t-test, error bars represent standard deviation, *$P < 0.05$, ***

441 $P < 0.001$.

Figure 4

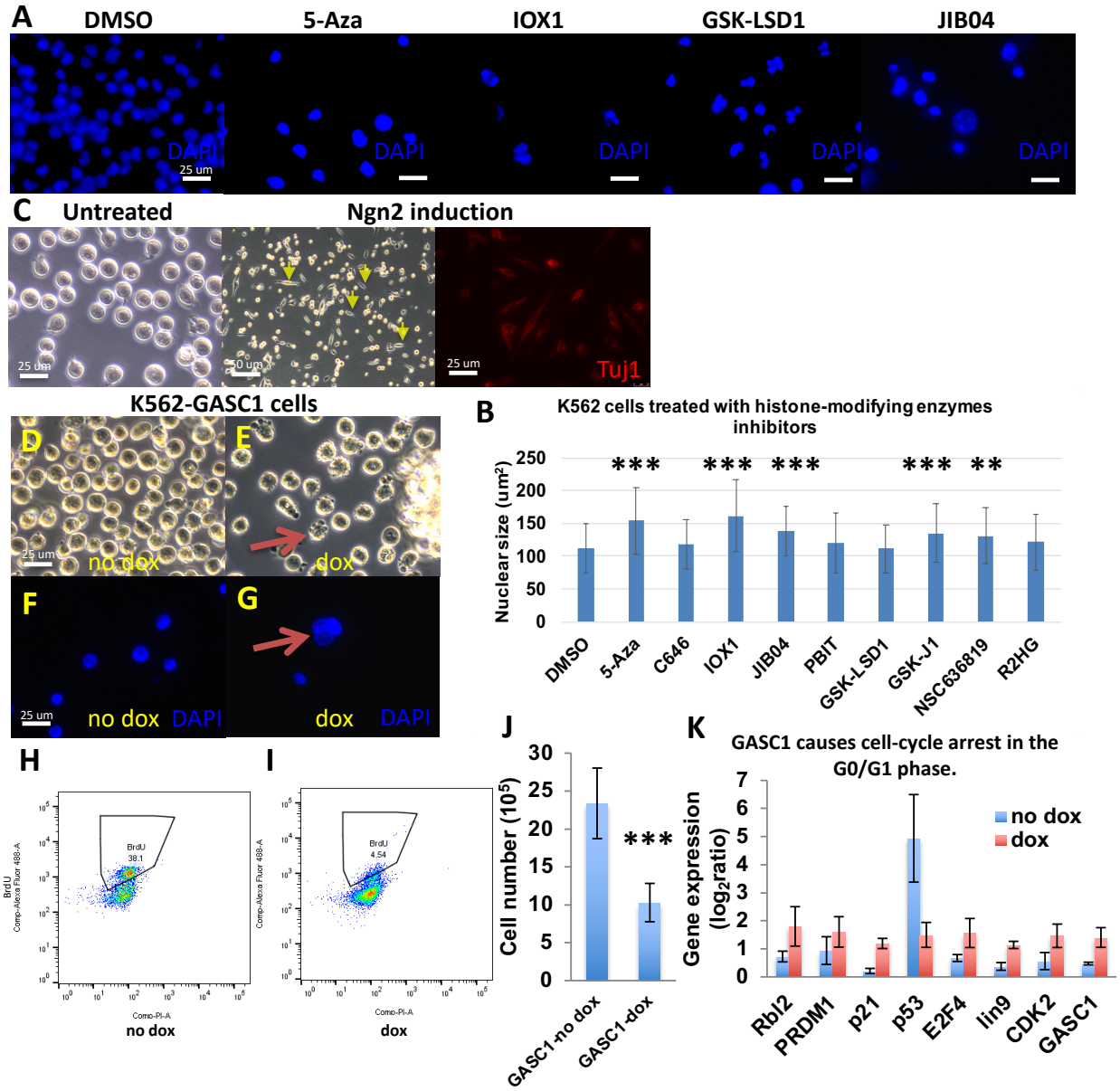

Fig. 4. GASC1 promotes aberrant nuclear structure and cell cycle arrest of leukemia cells. (*A*) Representative images of DAPI staining for K562 cells treated with DMSO as control and 5-Aza, IOX1, GSK-LSD1, and JIB04. It was shown that the bigger size and twisted shape of nuclei in inhibitors treatment. The images were taken at 40× on a confocal microscope. White scale bars= 25 μm.

448 **(*B*)** Measurements of the nuclear size using DAPI staining under fluorescence microscopy after
449 K562 cells treated with inhibitors of chromatin-modifying enzymes. Two-tailed t-test, Mean ± SD.
450 **P < 0.01, ***P < 0.001.
451 **(*C*)** Brightfield and fluorescent images show that K562 leukemia cells differentiate to iN cells with
452 Ngn2 overexpression after 14 days differentiation and stain with the neuronal marker Tuj1 (red),
453 compared to healthy and as cultured K562 cells without any treatment. The yellow arrows indicate
454 the cells of morphological changes.
455 **(*D* and *E*)** Brightfield images of K562 leukemia cells with induced expression of GASC1 with or
456 without doxycycline (dox). The no dox-induced GASC1 overexpression K562 cells show spherical
457 morphology, same as normal cells. The dox-induced GASC1 overexpression K562 cells show
458 morphology change from spherical to twisted shape and cell blebs. The red arrow indicates the
459 cells with twisted shapes and blebs. White scale bars= 25 μm.
460 **(*F* and *G*)** Fluorescent images by DAPI staining demonstrate that the dox-induced GASC1
461 overexpression K562 cells show the twisted nuclear shape and bigger nuclei compared with the no
462 dox-induced GASC1 overexpression K562 cells. The red arrow indicates the enlarged and twisted
463 nucleus. White scale bars= 25 μm.
464 **(*H* and *I*)** Flow cytometric analysis of K562 cells were double-stained with BrdU and PI. The dox-
465 induced GASC1 overexpression K562 cells proliferate significantly slower than the no dox-
466 induced GASC1 overexpression K562 cells by BrdU assay.
467 **(*J*)** Cell number counting after induction by dox for 7 days. The cell number is decreased in dox-

468 induced GASC1 overexpression K562 cells than no dox-induced GASC1 overexpression K562

469 cells. ***P < 0.001. n=3.

470 **(*K*)** The genes play a role in cell-cycle arrest detected by qPCR in the dox-induced GASC1

471 overexpression K562 cells and no dox-induced GASC1 overexpression K562 cells. Unpaired two-

472 tailed Student t-test. Data are mean ± SD. P < 0.001.

473 **REFERENCES**

474 1. A. C. Tamashunas *et al.*, High-throughput gene screen reveals modulators of nuclear shape.
475 *Mol Biol Cell* **31**, 1392-1402 (2020).
476 2. R. McBeath, D. M. Pirone, C. M. Nelson, K. Bhadriraju, C. S. Chen, Cell shape,
477 cytoskeletal tension, and RhoA regulate stem cell lineage commitment. *Dev Cell* **6**, 483-
478 495 (2004).
479 3. E. Bartova, J. Krejci, A. Harnicarova, S. Kozubek, Differentiation of human embryonic
480 stem cells induces condensation of chromosome territories and formation of
481 heterochromatin protein 1 foci. *Differentiation* **76**, 24-32 (2008).
482 4. J. D. Pajerowski, K. N. Dahl, F. L. Zhong, P. J. Sammak, D. E. Discher, Physical plasticity
483 of the nucleus in stem cell differentiation. *Proc Natl Acad Sci U S A* **104**, 15619-15624
484 (2007).
485 5. H. Shen, W. Xu, F. Lan, Histone lysine demethylases in mammalian embryonic
486 development. *Exp Mol Med* **49**, e325 (2017).
487 6. J. He *et al.*, Kdm2b maintains murine embryonic stem cell status by recruiting PRC1
488 complex to CpG islands of developmental genes. *Nat Cell Biol* **15**, 373-384 (2013).
489 7. J. D. Pereira *et al.*, Ezh2, the histone methyltransferase of PRC2, regulates the balance
490 between self-renewal and differentiation in the cerebral cortex. *Proc Natl Acad Sci U S A*
491 **107**, 15957-15962 (2010).
492 8. Y. H. Loh, W. Zhang, X. Chen, J. George, H. H. Ng, Jmjd1a and Jmjd2c histone H3 Lys 9
493 demethylases regulate self-renewal in embryonic stem cells. *Genes Dev* **21**, 2545-2557
494 (2007).
495 9. F. Kottakis *et al.*, NDY1/KDM2B functions as a master regulator of polycomb complexes
496 and controls self-renewal of breast cancer stem cells. *Cancer Res* **74**, 3935-3946 (2014).
497 10. I. Kupershmit, H. Khoury-Haddad, S. W. Awwad, N. Guttmann-Raviv, N. Ayoub, KDM4C
498 (GASC1) lysine demethylase is associated with mitotic chromatin and regulates
499 chromosome segregation during mitosis. *Nucleic Acids Res* **42**, 6168-6182 (2014).
500 11. Z. Q. Yang *et al.*, Identification of a novel gene, GASC1, within an amplicon at 9p23-24
501 frequently detected in esophageal cancer cell lines. *Cancer Res* **60**, 4735-4739 (2000).
502 12. P. A. Northcott *et al.*, Multiple recurrent genetic events converge on control of histone
503 lysine methylation in medulloblastoma. *Nat Genet* **41**, 465-472 (2009).
504 13. Z. Xiao *et al.*, GASC1 promotes glioma progression by enhancing NOTCH1 signaling.
505 *Mol Med Rep* **23**, (2021).
506 14. G. Liu *et al.*, Genomic amplification and oncogenic properties of the GASC1 histone
507 demethylase gene in breast cancer. *Oncogene* **28**, 4491-4500 (2009).
508 15. P. A. Cloos *et al.*, The putative oncogene GASC1 demethylates tri- and dimethylated lysine
509 9 on histone H3. *Nature* **442**, 307-311 (2006).
510 16. L. Wu *et al.*, Histone Demethylases KDM4A and KDM4C Regulate Differentiation of

511 Embryonic Stem Cells to Endothelial Cells. *Stem Cell Reports* **5**, 10-21 (2015).
512 17. H. Richly, L. Aloia, L. Di Croce, Roles of the Polycomb group proteins in stem cells and
513 cancer. *Cell Death Dis* **2**, e204 (2011).
514 18. S. J. Heo *et al.*, Differentiation alters stem cell nuclear architecture, mechanics, and
515 mechano-sensitivity. *Elife* **5**, (2016).
516 19. S. M. Chambers *et al.*, Highly efficient neural conversion of human ES and iPS cells by
517 dual inhibition of SMAD signaling. *Nat Biotechnol* **27**, 275-280 (2009).
518 20. Y. Zhang *et al.*, Rapid single-step induction of functional neurons from human pluripotent
519 stem cells. *Neuron* **78**, 785-798 (2013).
520 21. T. A. Volpe *et al.*, Regulation of heterochromatic silencing and histone H3 lysine-9
521 methylation by RNAi. *Science* **297**, 1833-1837 (2002).
522 22. K. K. Lee, J. L. Workman, Histone acetyltransferase complexes: one size doesn't fit all.
523 *Nat Rev Mol Cell Biol* **8**, 284-295 (2007).
524 23. A. D. Stephens *et al.*, Chromatin histone modifications and rigidity affect nuclear
525 morphology independent of lamins. *Mol Biol Cell* **29**, 220-233 (2018).
526 24. E. G. Fischer, Nuclear Morphology and the Biology of Cancer Cells. *Acta Cytol* **64**, 511-
527 519 (2020).
528 25. G. N. Papanicolaou, H. F. Traut, The diagnostic value of vaginal smears in carcinoma of
529 the uterus. 1941. *Arch Pathol Lab Med* **121**, 211-224 (1997).
530 26. T. Sullivan *et al.*, Loss of A-type lamin expression compromises nuclear envelope integrity
531 leading to muscular dystrophy. *J Cell Biol* **147**, 913-920 (1999).
532 27. L. Dang *et al.*, Cancer-associated IDH1 mutations produce 2-hydroxyglutarate. *Nature* **462**,
533 739-744 (2009).
534 28. C. Lu *et al.*, IDH mutation impairs histone demethylation and results in a block to cell
535 differentiation. *Nature* **483**, 474-478 (2012).
536 29. M. Koivomagi, M. P. Swaffer, J. J. Turner, G. Marinov, J. M. Skotheim, G1 cyclin-Cdk
537 promotes cell cycle entry through localized phosphorylation of RNA polymerase II.
538 *Science* **374**, 347-351 (2021).
539 30. J. A. Coffman, Cell cycle development. *Dev Cell* **6**, 321-327 (2004).
540 31. L. Litovchick *et al.*, Evolutionarily conserved multisubunit RBL2/p130 and E2F4 protein
541 complex represses human cell cycle-dependent genes in quiescence. *Mol Cell* **26**, 539-551
542 (2007).
543 32. G. Galiova, E. Bartova, I. Raska, J. Krejci, S. Kozubek, Chromatin changes induced by
544 lamin A/C deficiency and the histone deacetylase inhibitor trichostatin A. *Eur J Cell Biol*
545 **87**, 291-303 (2008).
546 33. P. Scaffidi, T. Misteli, Lamin A-dependent misregulation of adult stem cells associated with
547 accelerated ageing. *Nat Cell Biol* **10**, 452-459 (2008).
548 34. E. Meshorer *et al.*, Hyperdynamic plasticity of chromatin proteins in pluripotent embryonic
549 stem cells. *Dev Cell* **10**, 105-116 (2006).

550 35. E. Meshorer, T. Misteli, Chromatin in pluripotent embryonic stem cells and differentiation.
551 *Nat Rev Mol Cell Biol* **7**, 540-546 (2006).
552 36. C. Gurrion, M. Uriostegui, M. Zurita, Heterochromatin Reduction Correlates with the
553 Increase of the KDM4B and KDM6A Demethylases and the Expression of Pericentromeric
554 DNA during the Acquisition of a Transformed Phenotype. *J Cancer* **8**, 2866-2875 (2017).
555 37. B. E. Bernstein *et al.*, A bivalent chromatin structure marks key developmental genes in
556 embryonic stem cells. *Cell* **125**, 315-326 (2006).
557 38. T. S. Mikkelsen *et al.*, Genome-wide maps of chromatin state in pluripotent and lineage-
558 committed cells. *Nature* **448**, 553-560 (2007).
559 39. Y. Katoh, M. Katoh, Comparative integromics on JMJD2A, JMJD2B and JMJD2C:
560 preferential expression of JMJD2C in undifferentiated ES cells. *Int J Mol Med* **20**, 269-273
561 (2007).
562 40. T. Brambrink *et al.*, Sequential expression of pluripotency markers during direct
563 reprogramming of mouse somatic cells. *Cell Stem Cell* **2**, 151-159 (2008).
564 41. Z. P. Pang, P. Cao, W. Xu, T. C. Sudhof, Calmodulin controls synaptic strength via
565 presynaptic activation of calmodulin kinase II. *J Neurosci* **30**, 4132-4142 (2010).
566 42. M. Stadtfeld, N. Maherali, D. T. Breault, K. Hochedlinger, Defining molecular
567 cornerstones during fibroblast to iPS cell reprogramming in mouse. *Cell Stem Cell* **2**, 230-
568 240 (2008).
569 43. C. Chen, H. Okayama, High-efficiency transformation of mammalian cells by plasmid
570 DNA. *Mol Cell Biol* **7**, 2745-2752 (1987).

571